

SN 63



**PERFORMANCE PREDICTIONS
FOR AN SSME CONFIGURATION
WITH AN ENLARGED THROAT**

November 1985

(NASA-CR-178740) PERFORMANCE PREDICTIONS
FOR AN SSME CONFIGURATION WITH AN ENLARGED
THROAT (Software and Engineering Associates,
Inc.) 44 p HC AC3/MF A01 CSCL 21H

N86-21579

Unclas
G3/20 08803

Contract No. NAS8-35931

**By: G. R. Nickerson
L. D. Dang**

**Prepared For
George C. Marshall Space Flight Center
Marshall Space Flight Center, Al. 35812**



**Software And Engineering Associates, Inc.
1050 East William Street, Suite 402
Carson City, Nevada 89701**

TABLE OF CONTENTS

	<u>Page No.</u>
Nomenclature	iv
Abbreviations	v
1. Introduction	1
2. Performance Prediction Results	4
3. Factors Effecting the Performance Prediction Results	6
4. Comparison of Shock Results with other Computer Programs	10
5. Conclusions	12
5.1 Chemical Kinetics	12
5.2 Transonic Analysis	12
5.3 Shock Wave Prediction	13
5.4 Thrust Chamber Performance Prediction	13
6. Recommendations	14
References	34
Appendix A	36

LIST OF FIGURES

	<u>Page No.</u>
Figure 1: SSME Main Combustion Chamber (MCC)	15
Figure 2: A Comparison of Current and Large Throat SSME MCC/Nozzle Configurations	16
Figure 3: TDK Input for SSME Current Design Analysis	17
Figure 4: TDK Input for SSME "Large Throat" Design Analysis	18
Figure 5: SSME Wall Temperature	19
Figure 6: TDK Performance Summary for SSME Current Configuration	20
Figure 7: TDK Performance Summary for SSME "Large Throat" Configuration	21
Figure 8: Flow Velocity along a Gas Streamline Behind an Oblique Shock. SSME "Large Throat" Design	22
Figure 9: SSME Large Throat Design	23
Figure 10: Isomach from Throat Minimum Point for Back Nozzle	24
Figure 11: VNAP2 Isomach Predictions for the "Large Throat" SSME Design	25
Figure 12: VNAP2 Solution Grid	26
Figure 13: Sensitivity of Nozzle Mass Coefficient, C_D	27
Figure 14: Transonic Analysis	28
Figure 15: SSME Current Design, Induced Shock Predictions	29

LIST OF FIGURES

	<u>Page No.</u>
Figure 16: SSME "Large Throat" Design, Induced Shock Predictions	30
Figure 17: SSME Current Design, Shock angle vs x/r^*	31
Figure 18: SSME "Large Throat" Design, Shock angle vs x/r^*	31
Figure 19: Shock Strength vs x/r^* for Differing Transonic Start Lines	32
Figure 20: Summary of Shock Strength Predictions	33

851106

NOMENCLATURE

alphabetic

C_D	flow coefficient, nozzle mass flow/1-D mass flow
I_{sp}	specific impulse
$I_{sp, \text{theoretical}}$	specific impulse for an isentropic equilibrium expansion
M	Mach number
r	radial coordinate. $r=0$ at axis
r^*	throat radius
R	throat radius/ r^*
R_d	downstream throat radius/ r^*
R_u	upstream throat radius/ r^*
x	axial coordinate. $x=0$ at throat plane

Greek

β	angle between shock and gas streamline, shock strength (see page 4)
γ	ratio of specific heats
ϵ	nozzle expansion ratio
η_{DER}	Distributed Energy Release efficiency
$\eta_{TDK, BLM}$	aerodynamic efficiency, including chemical kinetics
θ	angle between gas streamline and axis
ϕ	angle between surface and axis

851106

ABBREVIATIONS

BLM	Boundary Layer Module, computer program
DER	Distributed Energy Release
JANNAF	Joint Army-Navy-NASA-Air Force
LRC	Left Running Characteristic
MCC	Main Combustion Chamber
MOC	Method of Characteristics
ODE	One-Dimensional Equilibrium Expansion
ODF	One-Dimensional Frozen Expansion
ODK	One-Dimensional Kinetics Expansion
RRC	Right Running Characteristic
SEA	Software and Engineering Associates, Inc.
SSME	Space Shuttle Main Engine
TDK	Two-Dimensional Kinetics, JANNAF computer program
VNAP2	Viscous Nozzle Analysis Program, Version 2

1. INTRODUCTION

-In--this study the Two-Dimensional Kinetics (TDK) computer program that has recently been developed for the NASA under contract NAS8 - 35931 was used to predict the performance of a "Large Throat Configuration" of the Space Shuttle Main Engine (SSME)⁽¹⁾. Calculations indicate that the current design SSME contains a shock wave that is induced by the nozzle wall shape⁽²⁾. In the "Large Throat" design an even stronger shock wave is predicted. Because of the presence of this shock wave, earlier performance predictions that have neglected shock wave effects have been questioned. In this study the JANNAF thrust chamber performance prediction procedures given in Reference 3 have been applied. The analysis includes the effects of two dimensional reacting flow with a shock wave. The effects of the boundary layer with a regeneratively cooled wall are also included. This analysis has been made possible by the development of a new shock wave version of the TDK computer program⁽¹⁾.

In order to substantiate the calculations, a computer program developed by Prof. Hoffman at Purdue University was also used⁽⁴⁾. The results were run independently at Purdue with input data supplied by SEA, Inc. The Purdue computer program can compute axially symmetric supersonic nozzle flows with an induced shock, but is restricted to flows with a constant ratio of specific heats, γ . Thus, the TDK program was also run with this assumption and the results of the two programs were compared.

851106

Nozzle Geometry and Operating Conditions

The Space Shuttle Main Engine (SSME) utilizes a thrust chamber that is constructed in two sections, 1) a Main Combustion Chamber (MCC) assembly, and 2) an expansion nozzle assembly. The MCC current design is shown in Figure 1. The nozzle assembly is bolted to the MCC at a nozzle attach flange. The nozzle expansion ratio at the attachment position is 5:1.

The "Large Throat" version of the SSME is constructed by modification of the MCC. The nozzle assembly is not modified. The current design and "Large Throat" design MCC geometries are compared in Figure 2. It can be seen that the enlargement of the nozzle throat reduces the nozzle expansion ratio from 77.5 to 69.5:1. The chamber pressure is reduced from 3285 (109% power level) to 3010 psia. The distance from the nozzle throat to the nozzle exit is very slightly decreased. There is a considerable difference in throat radius of curvature, both the upstream and downstream values, between the two designs.

Nozzle geometry and operating conditions for the SSME current design nozzle (109% power level) were obtained from NASA/MSFC and are given in Figure 3, which is an annotated listing of the input data. Definitions for all of the input data items are given in Reference 1. Those input items which were changed in order to run the "large throat" SSME are listed in Figure 4. The wall temperature profile for these engines is shown in Figure 5.

The calculations were made assuming that 1) there is perfect mixing so that the overall engine mixture ratio of 6.05485 is achieved, and 2) the system enthalpy is determined from tank conditions. These assumptions are equivalent to assuming that the distributed energy release efficiency, η_{DER} , is unity.

Results were then calibrated using measured data. That is, an actual value of η_{DER} was estimated from

$$I_{SP_{measured}} = \eta_{DER} \eta_{TDK, BLM} I_{SP_{theoretical}} \quad (1)$$

so that for the current design

$$I_{SP_{predict}} = I_{SP_{measured}} \quad (2)$$

The performance predictions results are presented in the next section.

2. PERFORMANCE PREDICTION RESULTS

Performance prediction results are summarized in Figures 6 and 7 for the current design and "Large Throat" designs, respectively. (See Appendix A for an explanation of these summary sheets). The measured I_{SP} for the current design is known to be 452.6 ± 1 seconds. The distributed energy release efficiency for the engine is found from equation (1) as follows:

$$I_{SP_{TDK, BLM}} = 458.0 \text{ sec.}$$

$$\eta_{TDK, BLM} = 458.0/465.1 = .9847$$

$$\eta_{DER} = .9882$$

Thus, it is predicted that the distributed energy release loss for this engine is 5.4 seconds. This value is consistent with the value of 5.3 seconds predicted by R. Carroll⁽⁶⁾ using a full distributed energy release analysis.

As can be seen from Figure 6, the maximum shock strength, β , predicted for the current design nozzle is .29. This value is taken at the intersection of the last Left Running Characteristic (LRC) surface and the shock surface. Downstream of this intersection the shock can not effect thrust chamber performance. Shock strength is defined here as

$$\beta = (P_2 - P_1) / P_1$$

where

P_1 is the pressure in front of the shock, and

P_2 is the pressure behind the shock.

851106

For the large throat design the maximum shock strength is found from Figure 7 to be 1.13. The difference in theoretical performance between the two engines is (ISP (ODE) values from Figure 6 and 7)

$$465.13 - 463.26 = 1.87 \text{ seconds.}$$

The difference in predicted performance is (ISP (TC) * η_{DER} from Figure 6 and 7)

$$452.6 - 449.1 = 3.5 \text{ seconds, (with } \eta_{DER} = .9882)$$

which is larger than expected. From the analysis presented here it appears that the lowered performance predicted for the "Large Throat" SSME design is almost entirely due to the effect of the shock wave calculation. Factors that influence the performance calculations are discussed in the next section.

3. FACTORS EFFECTING THE PERFORMANCE PREDICTION RESULTS

An examination of the computed results indicate that the lowered performance predicted for the "Large Throat" SSME is a result of the shock wave calculation. In order to minimize the numerical error contained in the calculation, an extremely fine mesh spacing was used. The number of points in the initial data line was set at 250. Each Method of Characteristics (MOC) flow field calculation was carried out using approximately 100,000 points.

Two phenomena were examined in detail: 1) the interaction of the shock wave with the chemical kinetics of the flow, and 2) the transonic flow field. Each is discussed below.

Shock Wave and Chemistry Interaction

Across the shock front, the translational degrees of freedom of a gas are equilibrated within a few molecular collisions*. The chemical composition of the gas is frozen during this time since thousands of molecular collisions are required for even the fastest chemical reactions. Thus a chemical excitation process can occur immediately behind the shock front. Since the kinetic rate equations are notoriously stiff, it is necessary that a fully implicit integration method be used (see Ref. 1, Section 3.1.1).

* The present analysis assumed that both the translational and vib.-rot. degrees of freedom are equilibrated across the shock.

In order to test the accuracy of the TDK integration procedure immediately behind a shock point, a streamline was selected from the "Large Throat" SSME TDK analysis. A pressure defined ODK calculation was then carried out for this streamline starting at the back side of the shock. The shock strength was 1.05, so that there was a considerable change in pressure and temperature across the shock.

A comparison of the TDK and ODK streamline calculations are shown in Figure 8. Each TDK mesh point is shown. The ODK integration step is approximately 1000 times smaller than the TDK mesh size. Never the less, the two results cannot be separated on the scale shown in the figure. Velocity vs path length was chosen since velocity is a direct measure of specific impulse (for one-dimensional flow, optimum $I_{sp} = V/g$). A computer generated plot repeating this result, but with higher resolution, is given in Figure 9. It can be concluded that for this case, TDK is giving an accurate result.

A one-dimensional frozen (ODF) calculation was also carried out for this streamline. There were no differences between the ODF and ODK results, i.e., the frozen and equilibrium paths were found to be the same. Thus, in this flow regime there can be no dissociation of H_2O or H_2 due to a shock of this strength. It follows that no significant energy can be bound up in dissociated species causing a performance loss. The shock wave and chemistry interaction is found to be negligible.

The Transonic Flow Field

The most important parameter effecting the transonic flow field is the radius of curvature immediately upstream of the

nozzle throat. This value was reduced from $R_u = 1$ in the current design to $R_u = .494$ in the "Large Throat" design (see Figure 2). The modified Sauer transonic analysis used by the TDK program is based on perturbation theory (see Reference 1, Section 2.4) and a value of $R_u = .494$ is at the lower limit for which the analysis has been validated. Because of this fact, the analysis was re-examined in order to assess its accuracy for calculating the MOC start line for the "Large Throat" SSME. In particular, results obtained from the analysis were compared with results obtained from the VNAP2 computer program ⁽⁷⁾. Two cases were examined in some detail.

The first case examined was the nozzle studied by L. Back, Reference 8, for which ample experimental data is available. The Back case is for air flow through a nozzle with a small, $R_u = .625$, radius of curvature throat. Results of the analysis are shown in Figure 10. It can be seen that both methods are in excellent agreement with the data in the region near the wall. Near the flow axis, the TDK analysis is in closer agreement with the data than the VNAP2 analysis. In general, VNAP2 predicts flow accelerations along the nozzle axis that are greater than seen experimentally (see Reference 8 for further data).

The second case examined is the "Large Throat" SSME design. Results of the VNAP2 analysis are shown in Figure 11. Included in Figure 11 is the isomach attached to the throat minimum point as calculated for this case by the TDK modified Sauer transonic analysis. It can be seen that the agreement between this isomach and the corresponding isomach computed by VNAP2 is very similar to that measured by Back, et.al., Figure 10. A grid spacing of 101x34 was used for the VNAP2 runs. The VNAP2 solution grid for the "Large Throat" SSME case is shown in Figure 12.

851106

For the prediction of rocket engine performance it is important to be able to accurately estimate the steady state mass flow rate. This parameter is both difficult to measure experimentally or to predict theoretically for nozzles with small throat radius of curvature. The mass flow coefficient, C_D , can be shown to be rather sensitive to the flow angle distribution within the nozzle. Consider the isomach attached to the throat minimum point for the Back case shown in Figure 10. For this surface ($M = 1.346$) the C_D depends only on the flow angle distribution, $\theta(r)$. The C_D will be maximized if the flow is normal to the surface (although this violates the wall boundary condition). On the other hand if the flow angle is parallel to the nozzle centerline, then the C_D is very much reduced. Figure 13 gives computer values for C_D for these two cases ($\theta = \phi - \frac{\pi}{2}$ and $\theta = 0$). Also given is the C_D corresponding to the flow angle distribution computed by the TDK modified Sauer method. This computed distribution has then been perturbed $\pm 10\%$ and values of C_D determined. It can be seen from Figure 13 that a 10% perturbation in flow angle distribution gives significant differences (.5 to .8%) in computed mass flux. Results obtained for C_D and for the isomach attached to the nozzle throat minimum point are shown in Figure 14.

From the results discussed above it is concluded that the TDK modified Sauer analysis is adequate for the present application.

851106

4. COMPARISON OF SHOCK RESULTS WITH OTHER COMPUTER PROGRAMS

The current design and "Large Throat" design nozzles were analyzed using a method of characteristics computer program with shock tracing that was developed by Hoffman⁽⁴⁾. This MOC computer code can only analyze nozzle flows where the ratio of specific heats, γ , is constant. A value of $\gamma=1.24$ was selected for the analysis since this closely approximates the equilibrium value found in the region of the shock, i.e., at $T = 2500$ °R. These same two cases were also run using the constant γ option of the TDK computer program. A comparison of results obtained are presented in Figures 15 through 20.

The nozzle contour for the current configuration of the SSME is shown in Figure 15. An induced shock wave is found by both the TDK computer program and the Hoffman computer program⁽⁴⁾, which is indicated in the Figures by the initials JDH. The corresponding plot for the "Large Throat" configuration of the SSME is shown in Figure 16.

A plot of shock strength along the shock path for the current configuration of the SSME is shown in Figure 17. The corresponding plot for the "Large Throat" configuration of the SSME is shown in Figure 18.

From the above figures it can be seen that the shock begins as a weak disturbance. The shock path follows a Right Running Characteristic (RRC) surface until $x/r^* = 4$ for the current design nozzle, and $x/r^* = 3$ for the "Large Throat" design nozzle. The shock wave then gains in strength until the last LRC surface in the nozzle is reached. Downstream of this

position the shock cannot effect nozzle performance.

It was found that the shock strength calculation is sensitive to the input parameters. A sensitivity study was therefore carried out by J. D. Hoffman using the computer program described in Reference 4. The number of points on the initial data line was varied by doubling the spacing as follows: 21, 41, 81, and 161. The computed values of shock strength vs position are shown in Figure 19. The Hoffman program uses the modified Hall method⁽⁹⁾ for transonic analysis in constructing the initial data line. In order to determine the effect on shock strength of the transonic analysis, an initial data line calculated by TDK using the modified Sauer method was input into Hoffman's program. The results are also shown in Figure 19.

A sensitivity study was also carried by SEA using the TDK computer program. The purpose of the study was to examine the sensitivity of the performance calculation to the pressure calculation behind the shock front. It was found that a 1% error in pressure corresponds to roughly .75 seconds in specific impulse.

The Lockheed MOC program⁽¹⁰⁾ was also used to calculate the induced shock wave in these nozzles. Both Lockheed Huntsville, and Rocketdyne, used their version of the program to perform the calculations. Equilibrium chemistry was assumed. The results of all of these calculations are summarized in Figure 20.

5. CONCLUSIONS

As a result of the studies described in this report, the following conclusions are given regarding the performance of the SSME engine designs.

5.1 Chemical Kinetics

The effects of chemical kinetics are not important. The difference in predicted specific impulse between the ODE and ODK analysis is only 2/10 seconds. It is also shown that the shock waves found in the nozzles do not produce a kinetic loss. There is no significant difference between equilibrium and frozen gas properties in the region of the shock. A Mach shock would be required to activate the flow reaction chemistry.

5.2 Transonic Analysis

Three different transonic methods were used to obtain start lines for the MOC calculations, 1) modified Sauer⁽¹⁾, 2) modified Hall⁽⁹⁾, and 3) a time dependant finite difference method⁽⁷⁾. Each method produced a somewhat different shock wave solution. It is not possible to determine which transonic analysis is the more accurate. The modified Sauer analysis gives the best prediction of measured data⁽⁸⁾. The VNAP2 analysis, however, is based on more advanced methods. A nozzle design should be suspect if it shows a significant shock wave based on calculations using any one of these transonic methods. If the shock wave becomes sufficiently strong, e.g., $\beta > 1$, then according to the TDK computer program the nozzle performance is significantly degraded.

851106

5.3 Shock Wave Prediction

As shown in Figure 20, nozzle flow field calculations were carried out independently by several contractors. Each analysis predicted the existence of a shock wave in both the current and "Large Throat" SSME nozzle configurations. The SEA prediction gave a shock strength for the "Large Throat" nozzle that was 2.7 times as strong as in the current SSME design (see column 1 of Figures 6 and 7). Changes either in the transonic method, or in the MOC grid spacing were found to affect the shock strength as much as 50%, however, the predicted performance of the nozzles was little affected.

5.4 Thrust Chamber Performance Prediction

The analysis implies that for the current design SSME thrust chamber, the performance loss due to Distributed Energy Release is more than 5 seconds of specific impulse. If this is true, then improvement of the injector design could recover most of this performance loss.

The TDK computer program predicts a substantial* performance loss for the "Large Throat" SSME configuration, as compared to the current design. The loss appears to be primarily due to flow divergence, rather than shock wave effects. Because of the small downstream throat radius ($R_d = .2$) of the "Large Throat" SSME a finely spaced MOC grid is required near the wall to obtain an accurate performance prediction. The numerical accuracy of the performance predictions require further investigation.

The calculations indicate that a weak shock has little effect on performance, but a stronger shock ($\beta \sim 1$) can have an important effect on performance. The "Large Throat" SSME configuration appears to be near the threshold where shock wave effects become important.

* Loss due to nozzle aerodynamics = $3.5 - 1.9 = 1.6$ seconds.

See Section 2. (Aerodynamic Loss Includes: Divergence with Shocks and Boundary Layer Effects)

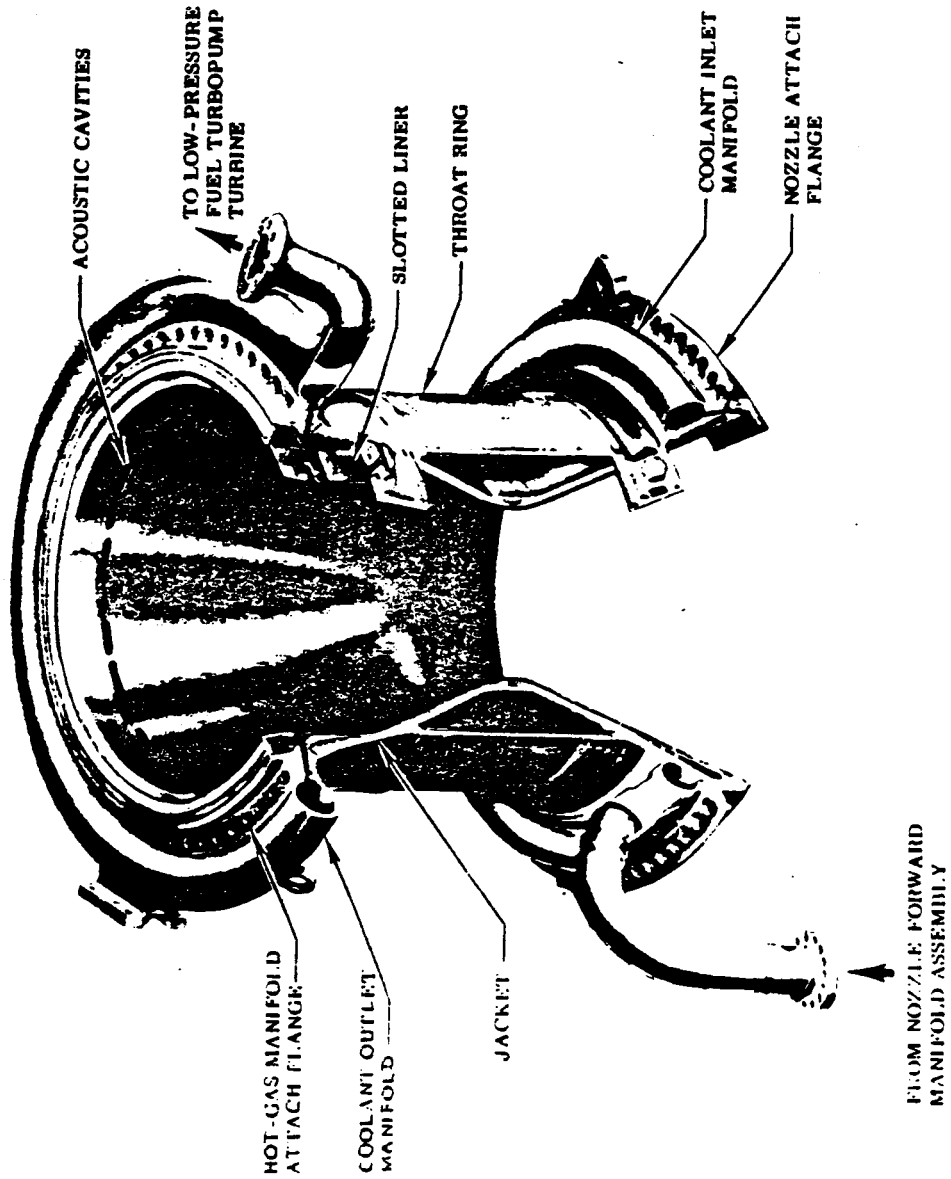
6. RECOMMENDATIONS

It is recommended that the SSME MCC be recontoured to reduce or eliminate the shock wave predicted for the "Large Throat" SSME design. This has recently been done by Rocketdyne (11,12) by replacing the contour downstream of the nozzle throat with a shape designed with the aid of a Rao method⁽¹³⁾ computer program. The revised contour was run by SEA, Inc. using the TDK computer program, which showed the nozzle to be shock free. The predicted nozzle performance was increased by .3 seconds.

With regard to a projected "Large Throat" SSME test program, the measurement of the shock location in the exit plane is recommended. A comparison of the predicted with the measured value will contribute significantly to verify the current analytical calculation method.

851106

ORIGINAL PAGE IS
OF POOR QUALITY



Geometry

Number of Acoustic Cavities	30
Injector End Diameter, inches	17.74
Throat Area, sq in.	83.41
Injector End to Throat Length, inches	14.00
Contraction Ratio	2.96:1
Expansion Ratio	5.0:1

Figure 1: SSME Main Combustion Chamber (MCC)

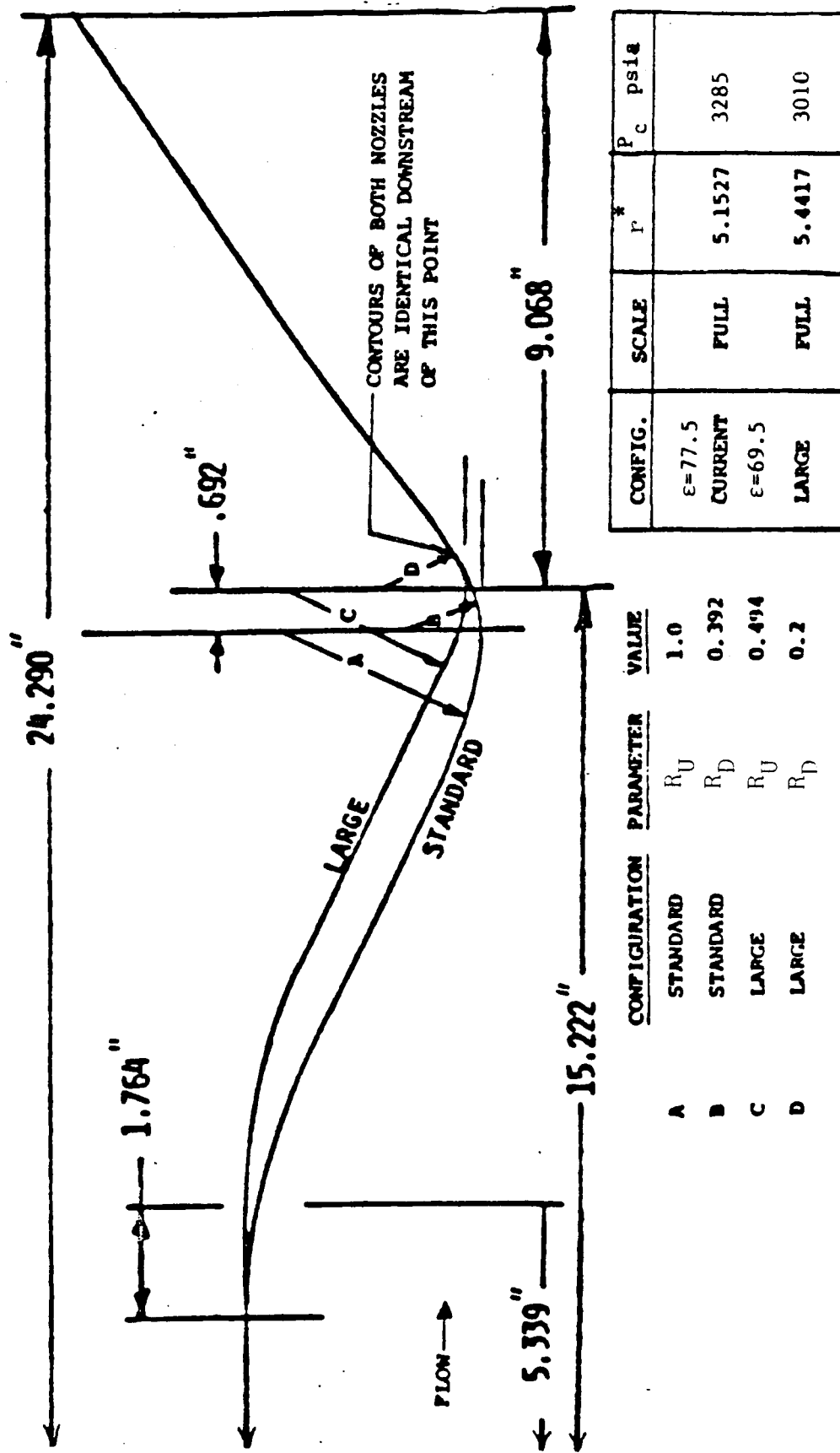


FIGURE 2: A COMPARISON OF CURRENT AND LARGE THROAT SSEE NOZZLE CONFIGURATIONS

TITLE SSME - COOLED WALL , CURRENT DESIGN, 10%

ORIGINAL PAGE IS
OF POOR QUALITY

DATA

\$DATA

COE = 1, OOK = 1, TDK = 1, BLM = 1, IRSTRT = 0,
SHOCK = 1,
IRPEAT = 1,
NZONES = 1,
ECRAT=3, ASUB=3,2,1.5, NASUB=3,
ASUP = 5,10,20,30,40,50,60,77.5, NASUP=8,
RSI = 5.1527, RTWU = 1, RWTD = .392, THETA = 25.4167, RI = 1.73921,
IWALL=4, THE=5.3748, THETA=37,
NWS = 18,

RS = 0, 1.126405, 1.173862, 1.255959, 1.379498, 1.551987,
1.741611, 1.947049, 2.186550, 2.212090, 2.226684,
2.363046, 3.785419, 5.338208, 6.586136, 7.564615,
8.298253, 8.803421,
ZS = 0, .2990952, .3626237, .4733999, .6422291, .8823416,
1.152396, 1.452449, 1.812502, 1.851582, 1.873954,
2.085214, 4.546562, 7.947338, 11.54691, 15.34513,
19.34211, 23.52318,

Thrust Chamber
Geometry

IOFF = 3,

\$END

REACTANTS

H 2.

100. -2154. L 20.27F
100. -3102. L 90.180

Tank Conditions
CPIA 246

O 2.

NAMELISTS

\$ODE

RKT = T,

P = 3285., XP = 1, PSIA = T, DELH = 0,

OFSKED = 6.05485,

\$END

REACTIONS

H + OH = H2O ,M1,A=7.5E23 ,N=2.6,B=0., (AR) NO. 1
O + H = OH ,M2,A=4.0E18 ,N=1.,B=0., (AR) NO. 2
O + O = O2 ,M3,A=1.2E17 ,N=1.,B=0., (AR) NO. 3
H + H = H2 ,M4,A=6.4E17 ,N=1.,B=0., (AR) NO. 6

END TBR REAX

H2 + OH = H + H2O ,A=2.19E13,N=0.,B=5.15, BAULCH(68)L2
OH + OH = O + H2O ,A=5.75E12,N=0.,B=.78, BAULCH(68)L2
H + OH = O + H2 ,A=7.33E12,N=0.,B=7.3, BAULCH(68)L2
O + OH = H + O2 ,A=1.3E13,N=0.,B=0., BAULCH(69)L3

Finite Rate
Chemistry

LAST REAX

THIRD BODY REAX RATE RATIOS

M1=20*H2O,5*H2,5*O2,12.5*H,12.5*O,12.5*OH,
M2=5*H2O,5*H2,5*O2,12.5*H,12.5*O,12.5*OH,
M3=5*H2O,5*H2,4.5*O2,12.5*H,12.5*O,12.5*OH,
M4=20*H2O,4*H2,1.5*O2,25*H,25*O,25*OH,

LAST CARD

\$OOK

JPRNT=-2,

EP = 77.5,

\$END

\$TRANS

MP = 250,

XM = 1,

\$END

\$MOC

NC = 0,

ISHCK=1,

IMAX=40, IMAXF=1,

\$END

\$BLM

OFC = 2, 2, DISTRB = 0, 0,

XCO = -2.4842, 1.85,

XCE = 1.849, 23.5,

IHFLAG = 0,

NTQW = 27,

XTQW = -2.4842, -2.1348, -1.9407, -1.7467, -.9704, -.7763, -.3881,
-.1941, .1941, .3881, .9704, 1.5526, 1.9407, 1.9601, 3.8815,
5.8222, 6.7926, 7.7629, 8.7333, 9.7037, 11.6444, 13.585,
15.5258, 17.4666, 19.4073, 21.3480, 23.523178,

TQW = 1360, 1500, 1510, 1500, 1470, 1470, 1490, 1490, 840, 830,
820, 790, 760, 1450, 1260, 1060, 960, 890, 850, 830, 795,
765, 745, 730, 720, 715, 710,

Wall
Temperature
°R

NTR = 10,

XINO = -2.4842, -2.40, -2.30,

RINO = 3*1.73251,

UEO = 535, 690.8, 979.2,

TEO = 6499.7, 6496.8, 6489.5,

PEO = 2918.1, 2906.3, 2877,

NSEGS = 6,

XSEG = -2.5, -.4658, .4658, 4.6578, 9.3155, 16.3021, 23.53,

APROF = 50, 76, NPROF = 0,

KDTPLT=0, KMTPLT=0, KTWPLT=0,

\$END

Figure 3: TDK Input for SSME Current Design Analysis

TITLE SSME - LARGE THROAT DESIGN, COOLED WALL
DATA

\$DATA
 ODE = 1, OOK = 1, TDK = 1, BLM = 1, IRSTRT = 0,
 SHOCK = 1,
 IRPEAT = 1,
 NZONES = 1,
 ECRAT=2.7, ASUB=2.7,2,1.5, NASUB=3,
 ASUP = 5,10,20,30,40,50,60,69.5, NASUP=8,
 RSI = 5.4417, RWU = .494, RWTD = .2, THETA = 25.4167, RI = 1.73921,
 IWALL=4,
 RS =1.066583 1.111520 1.189257
 1.306235 1.469563 1.649117 1.843644 2.070426
 2.094609 2.108428 2.237548 3.584382 5.054705
 6.236357 7.162870 7.857546 8.335885
 ZS =0.1560446 0.2161992 0.3210922
 0.4809552 0.7083157 0.9640279 1.248146 1.589077
 1.626081 1.647265 1.847305 4.177936 7.398101
 10.80651 14.40301 18.18771 22.14673
 NWS = 17,
 THE = 5.374800
 THETA = 37,
 IOFF = 3,
 SEND

REACTANTS
 H 2. 100. -2154. L 20.27F
 O 2. 100. -3102. L 90.180

NAMELISTS

\$OOE
 RKT = T,
 P = 3010., XP = 1, PSIA = T, DELH = 0,
 OFSKED = 6.05485,
 SEND

REACTIONS

H + OH = H2O	,M1,A=7.5E23 ,N=2.6,B=0.,	(AR) NO. 1
O + H = OH	,M2,A=4.0E18 ,N=1.,B=0.,	(AR) NO. 2
O + O = O2	,M3,A=1.2E17 ,N=1.,B=0.,	(AR) NO. 3
H + H = H2	,M4,A=6.4E17 ,N=1.,B=0.,	(AR) NO. 6

END TBR REAX

H2 + OH = H + H2O	,A=2.19E13,N=0.,B=5.15,	BAULCH(68)L2
OH + OH = O + H2O	,A=5.75E12,N=0.,B=.78,	BAULCH(68)L2
H + OH = O + H2	,A=7.33E12,N=0.,B=7.3,	BAULCH(68)L2
O + OH = H + O2	,A=1.3E13,N=0.,B=0.,	BAULCH(69)L3

LAST REAX

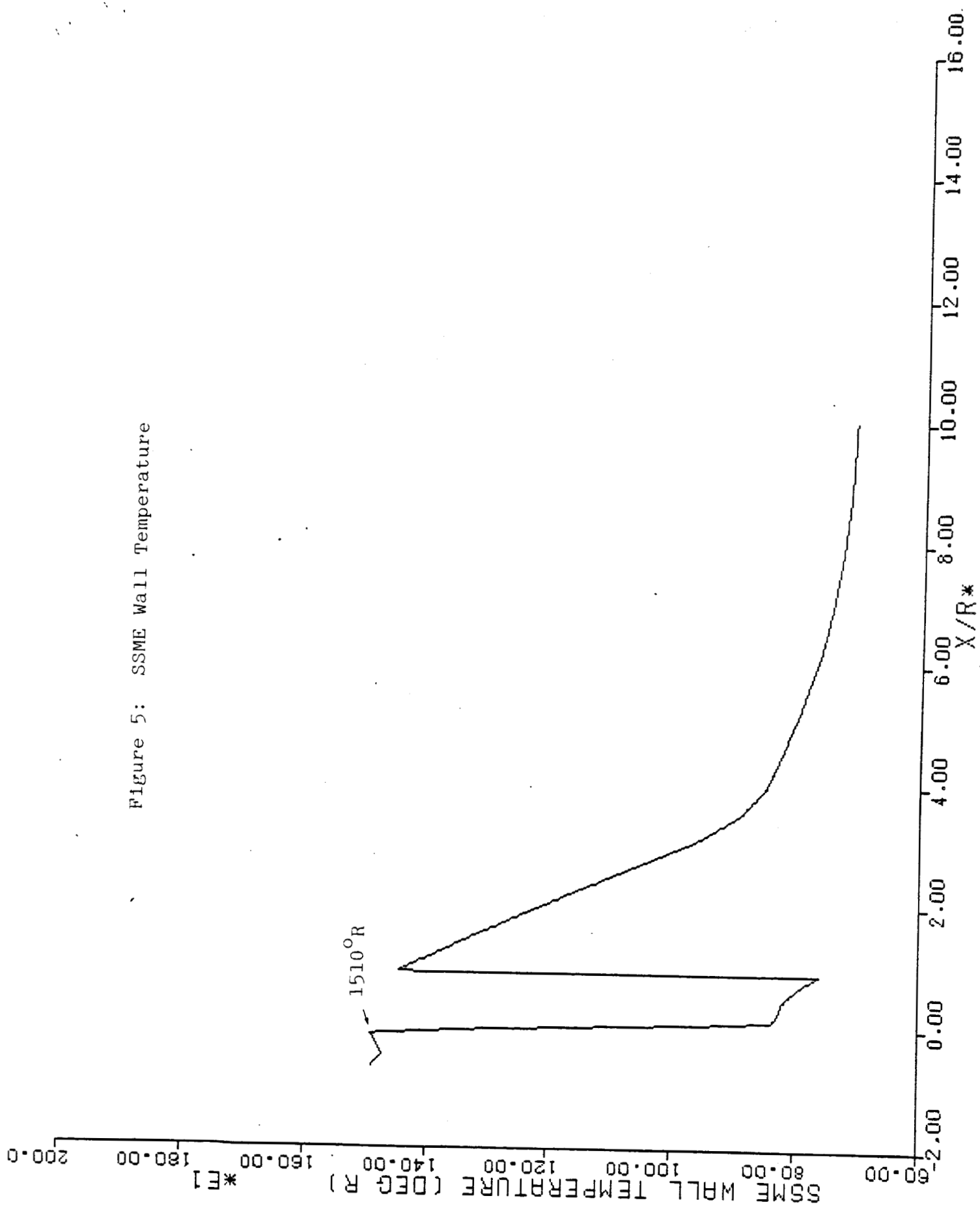
THIRD BODY REAX RATE RATIOS
 M1=20*H2O,5*H2,5*O2,12.5*H,12.5*O,12.5*OH,
 M2=5*H2O,5*H2,5*O2,12.5*H,12.5*O,12.5*OH,
 M3=5*H2O,5*H2,4.5*O2,12.5*H,12.5*O,12.5*OH,
 M4=20*H2O,4*H2,1.5*O2,25*H,25*O,25*OH,

LAST CARD

\$OOK
 JPRNT=-2,
 EP = 69.5,
 SEND
 \$TRANS
 MP = 250,
 XM = 1,
 SEND
 NC=0,
 IMAX=40, IMAXF=1,
 ISHCK=2,
 SEND
 \$BLM
 IHFLAG = 0,
 OFC = 2, 2, DISTRB = 0, 0,
 XCO = -2.4842, 1.85,
 XCE = 1.849, 22.15,
 NTR = 10,
 XINO = -2.5, -2.40, -2.30,
 RINO = 3*1.6432,
 UEO = 535, 690.8, 979.2,
 TEO = 6499.7, 6496.8, 6489.5,
 PEO = 2918.1, 2906.3, 2877,
 NSEGS = 6,
 XSEG = -2.5, -.4658, .4658, 4.6578, 9.3155, 16.3021, 22.16,
 APROF = 50, 76, NPROF = 0,
 KDTPLT=0,KMTPLT=0,KTWPLT=0,
 NTQW = 27,
 XTQW = -2.4842, -2.1348, -1.9407, -1.7467, -.9704, -.7763, -.3881,
 -.1941, .1941, .3881, .9704, 1.5526, 1.9407, 1.9601, 3.8815,
 5.8222, 6.7926, 7.7629, 8.7333, 9.7037, 11.6444, 13.585,
 15.5258, 17.4666, 19.4073, 21.3480, 23.523178,
 TQW = 1360, 1500, 1510, 1500, 1470, 1470, 1490, 1490, 840, 830,
 820, 790, 760, 1450, 1260, 1060, 960, 890, 850, 830, 795,
 765, 745, 730, 720, 715, 710,
 SEND

Figure 4: TDK Input for SSME "Large Throat" Design Analysis

Figure 5: SSME Wall Temperature



TDK PERFORMANCE SUMMARY : SSME - COOLED WALL , CURRENT DESIGN, 109%
 REAL WALL CONTOUR 1 ZONES WALL TEMP

		FIRST TDK/BLM SOLUTION	SECOND TDK/BLM SOLUTION
THRUST CHAMBER OPERATING CONDITIONS			
CHAMBER PRESS	[PSIA]	3285.000	3285.000
CHAMBER TEMP	[R]	6543.192	6609.458
MIXTURE RATIO	[-]	6.054850	6.054850
H (OXID)	[CAL/MOLE]	-3102.000	-3102.000
H (FUEL)	[CAL/MOLE]	-2154.000	-2154.000
HCHAM (ODE)	[BTU/LB]	-422.3787	-303.6657
DELH (AVERAGE)	[BTU/LB]	0.0000000E+00	0.0000000E+00
DELH1 (AVE)	[BTU/LB]	0.0000000E+00	118.7092
THRUST CHAMBER GEOMETRY			
ECRAT	[-]	3.000000	2.997371
RI	[-]	1.739210	1.739210
THETA1	[DEGREES]	25.41670	25.41670
RWTU	[-]	1.000000	0.9985945
RSTAR	[INCHES]	5.152700	5.156323
RWTD	[-]	0.3920000	0.3910218
NIT	[-]	243.0000	243.0000
THE	[DEGREES]	5.374800	5.299142
THETA	[DEGREES]	37.00000	37.00000
EP (NOZZLE)	[-]	77.50022	76.50255
SHOCK PARAMETERS			
XA (X/R*)	[-]	0.2359115	0.2359115
XB (X/R*)	[-]	0.0000000E+00	0.0000000E+00
SHOCK (R/R*)	[-]	2.584894	2.589131
SHOCK (X/R*)	[-]	8.834632	8.839259
SHOCK STRENGTH	[-]	0.2892100	0.0000000E+00
EXIT FLOW PROPERTIES			
P (AXIS,EXIT)	[PSIA]	0.2726767	0.2756312
P (WALL,EXIT)	[PSIA]	6.109700	6.161937
T (WALL,EXIT)	[R]	2483.953	2561.766
V (WALL,EXIT)	[FT/SEC]	14039.21	14149.57
MA (WALL,EXIT)	[-]	4.271464	4.243621
ONE-DIMENSIONAL FLOW PERFORMANCE			
ISP (ODE)	[SECONDS]	465.1311	469.2740
ISP (ODK)	[SECONDS]	464.9658	469.0910
ISP (ODF)	[SECONDS]	446.7661	449.4862
TWO-DIMENSIONAL FLOW PERFORMANCE			
CD	[-]	0.9896466	0.9910184
CF (TDK)	[-]	1.921868	1.928235
CSTAR (TDK)	[FT/SEC]	7713.456	7768.724
THRUST (TDK)	[POUNDS]	526597.2	528341.6
WDOT (TDK)	[LB/SEC]	1142.907	1136.373
ISP (TDK)	[SECONDS]	460.7523	464.9368
BOUNDARY LAYER PARAMETERS			
DFOPT (BLME)	[POUNDS]	8386.935	8285.425
DF (BLME)	[POUNDS]	7931.962	7829.081
DISP (BLME)	[SECONDS]	6.940162	6.889535
THETA (EXIT)	[FEET]	0.1777533E-01	0.1777533E-01
DEL* (EXIT)	[FEET]	0.2187267E-01	0.2187267E-01
EP (REGEN)	[BTU/SEC]	77.46112	77.46112
SQDOT (REGEN)	[BTU/SEC]	135682.6	0.0000000E+00
SQDOT (LOSS)	[BTU/SEC]	56.39063	56.39063
THRUST CHAMBER PERFORMANCE			
THRUST (TC)	[POUNDS]	518665.2	520512.5
ISP (TC)	[SECONDS]	453.8121	458.0472
CF (TC)	[-]	1.892919	1.899662

Figure 6: TDK Performance Summary for SSME Current Configuration

TDK PERFORMANCE SUMMARY : SSME - LARGE THROAT DESIGN, COOLED WALL
 REAL WALL CONTOUR 1 ZONES WALL TEMP
 INDUCED SHOCK AFTER XA

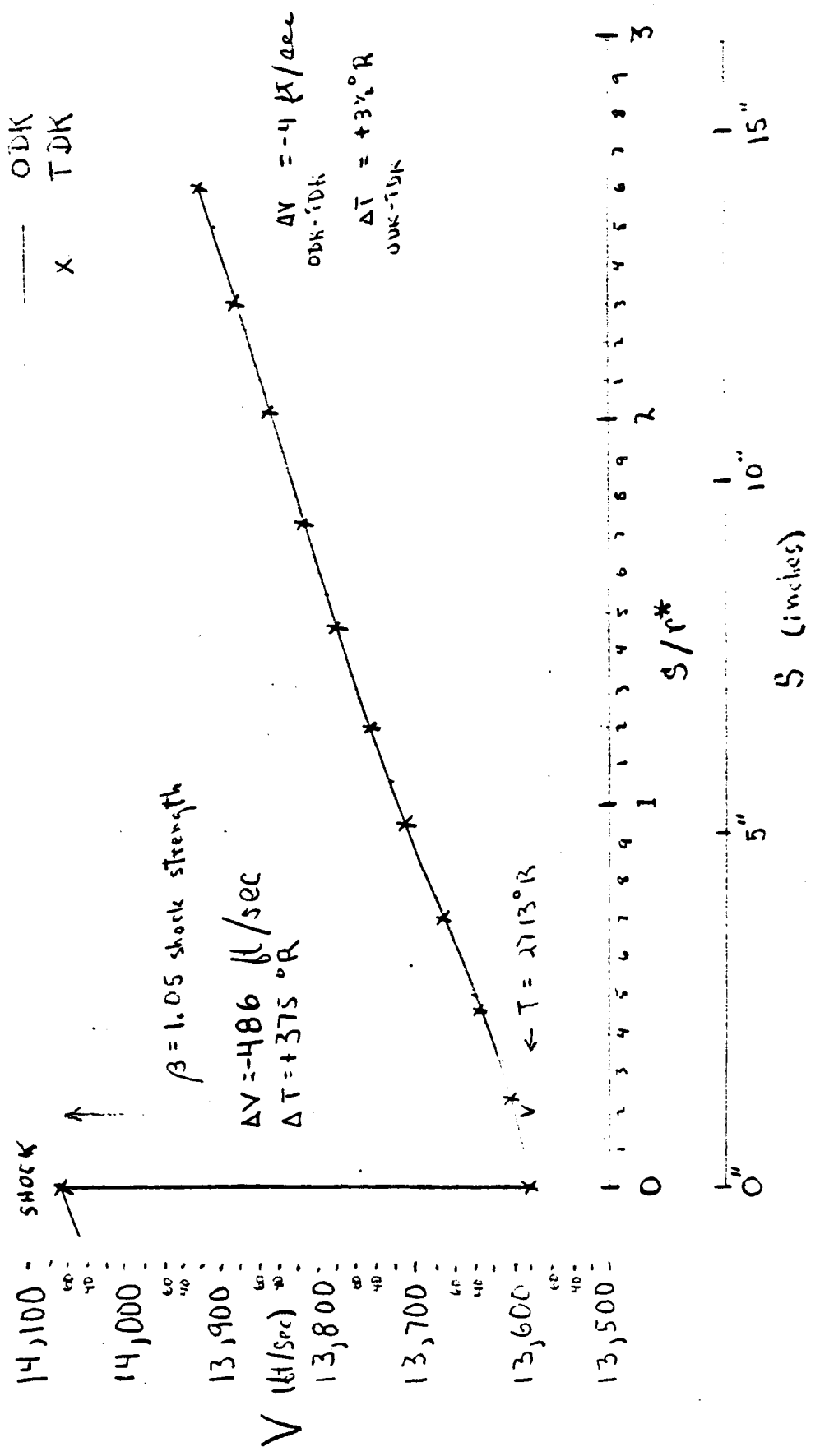
		FIRST TDK/BLM SOLUTION	SECOND TDK/BLM SOLUTION
THRUST CHAMBER OPERATING CONDITIONS			
CHAMBER PRESS	[PSIA]	3010.000	3010.000
CHAMBER TEMP	[R]	6526.882	6591.104
MIXTURE RATIO	[-]	6.054850	6.054850
H (OXID)	[CAL/MOLE]	-3102.000	-3102.000
H (FUEL)	[CAL/MOLE]	-2154.000	-2154.000
HCHAM (ODE)	[BTU/LB]	-422.3749	-305.6916
DELH (AVERAGE)	[BTU/LB]	0.0000000E+00	0.0000000E+00
DELH1 (AVE)	[BTU/LB]	0.0000000E+00	116.6856
THRUST CHAMBER GEOMETRY			
ECRAT	[-]	2.700000	2.694912
RI	[-]	1.739210	1.739210
THETA1	[DEGREES]	25.41670	25.41670
RWTU	[-]	0.4940000	0.4925624
RSTAR	[INCHES]	5.441700	5.446941
RWTD	[-]	0.2000000	0.1988453
NIT	[-]	244.0000	244.0000
THE	[DEGREES]	5.374800	5.327114
THETA	[DEGREES]	37.00000	37.00000
EP (NOZZLE)	[-]	69.48698	68.57317
SHOCK PARAMETERS			
XA (X/R*)	[-]	0.1203630	0.1203630
XB (X/R*)	[-]	0.0000000E+00	0.0000000E+00
SHOCK (R/R*)	[-]	2.637427	2.612652
SHOCK (X/R*)	[-]	8.547814	8.626249
SHOCK STRENGTH	[-]	1.131168	1.138703
EXIT FLOW PROPERTIES			
P (AXIS,EXIT)	[PSIA]	0.2820055	0.2786561
P (WALL,EXIT)	[PSIA]	6.195770	6.247626
T (WALL,EXIT)	[R]	2519.777	2589.486
V (WALL,EXIT)	[FT/SEC]	13992.76	14109.94
MA (WALL,EXIT)	[-]	4.229021	4.210537
ONE-DIMENSIONAL FLOW PERFORMANCE			
ISP (ODE)	[SECONDS]	463.2604	467.2708
ISP (OOK)	[SECONDS]	463.0793	467.0724
ISP (ODF)	[SECONDS]	444.7228	447.3469
TWO-DIMENSIONAL FLOW PERFORMANCE			
CD	[-]	0.9802917	0.9821196
CF (TDK)	[-]	1.892262	1.898804
CSTAR (TDK)	[FT/SEC]	7774.756	7830.471
THRUST (TDK)	[POUNDS]	529866.9	531698.8
WDOT (TDK)	[LB/SEC]	1158.788	1152.760
ISP (TDK)	[SECONDS]	457.2597	461.2397
BOUNDARY LAYER PARAMETERS			
DFOPT (BLME)	[POUNDS]	8341.068	8277.303
DF (BLME)	[POUNDS]	7889.169	7824.075
DISP (BLME)	[SECONDS]	6.808123	6.787252
THETA (EXIT)	[FEET]	0.1780233E-01	0.1780233E-01
DEL* (EXIT)	[FEET]	0.2142398E-01	0.2142398E-01
EP (REGEN)	[BTU/SEC]	69.48714	69.48714
SQDOT (RE:EN)	[BTU/SEC]	135283.0	0.0000000E+00
SQDOT (LOSS)	[BTU/SEC]	0.0000000E+00	0.0000000E+00
THRUST CHAMBER PERFORMANCE			
THRUST (TC)	[POUNDS]	521977.8	523874.7
ISP (TC)	[SECONDS]	450.4516	454.4525
CF (TC)	[-]	1.864088	1.870862

Figure 7: TDK Performance Summary for SSME "Large Throat" Configuration

SSME LARGE THROAT DESIGN

V vs S Behind Shocks

ODK & TDK



ORIGINAL PAGE IS OF POOR QUALITY

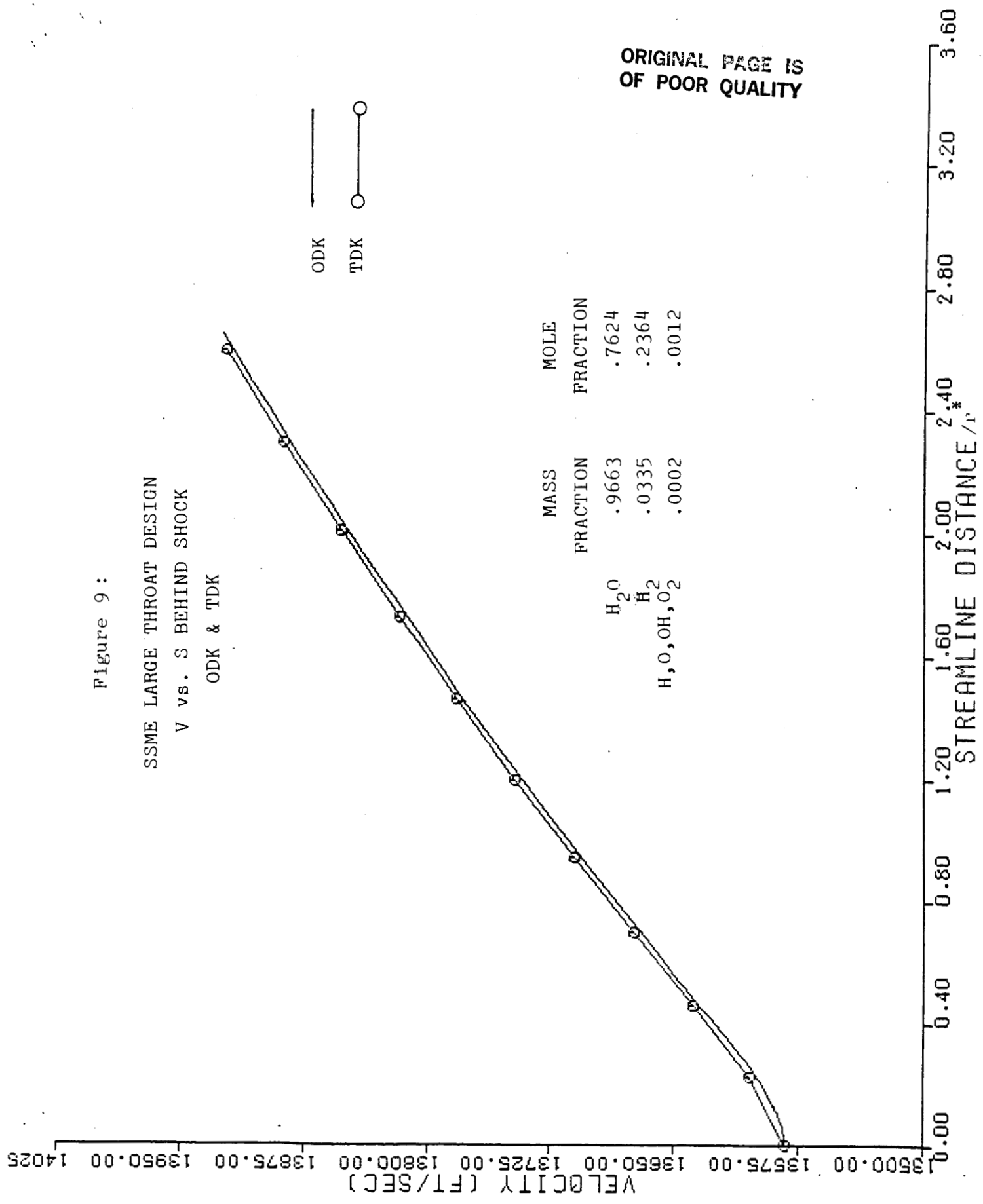
Figure 8: Flow Velocity along a Gas Streamline Behind an Oblique Shock. SSME "Large Throat" Design

ORIGINAL PAGE IS
OF POOR QUALITY

Figure 9:

SSME LARGE THROAT DESIGN
V vs. S BEHIND SHOCK
ODK & TDK

ODK ———
TDK ○—○



TRANSONIC SOLUTION
COMPARISON WITH DATA

MEASURED	C_D
MOD. SAUER	.985
CD	.985
VNAP2	.982
CD	.982

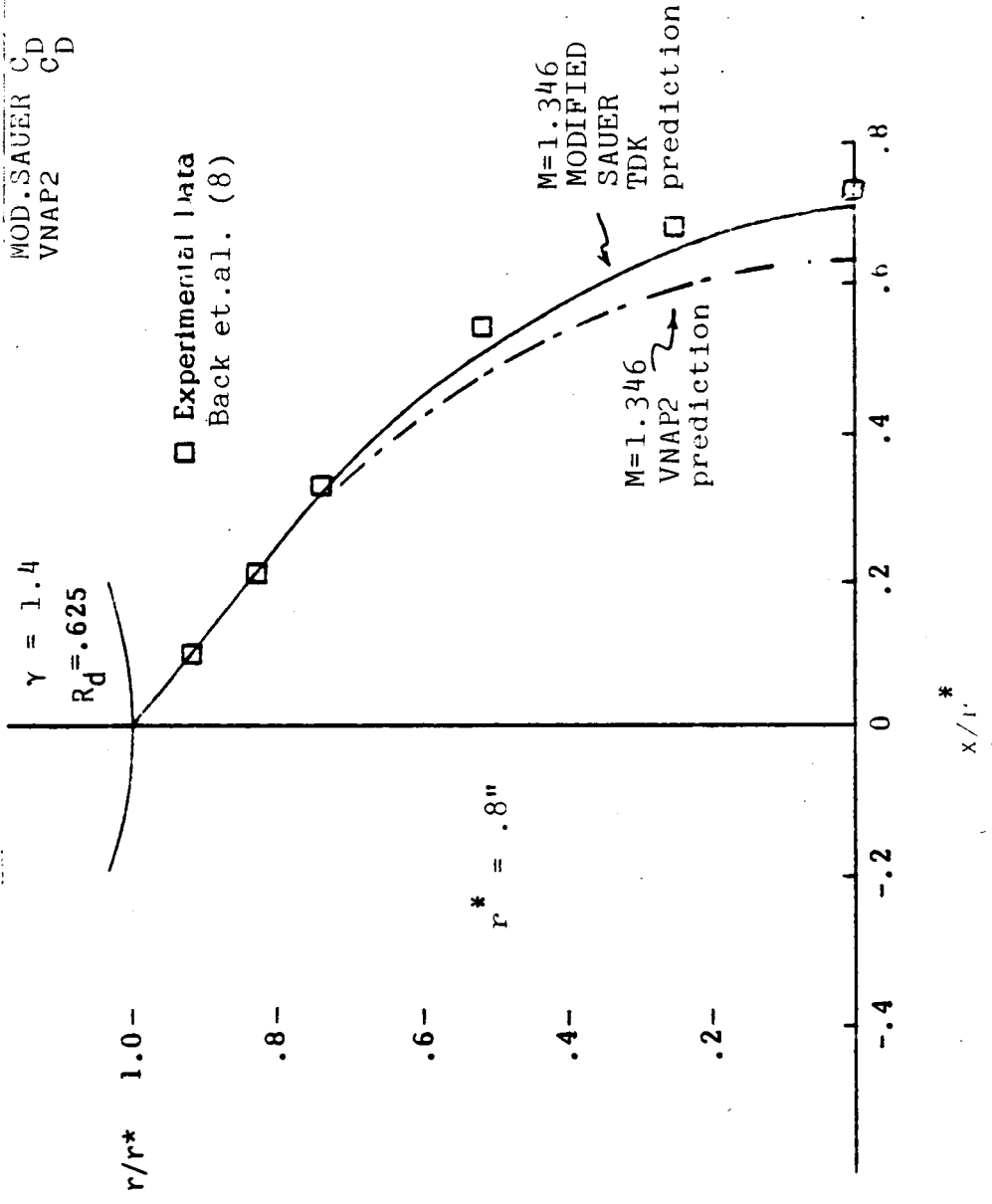
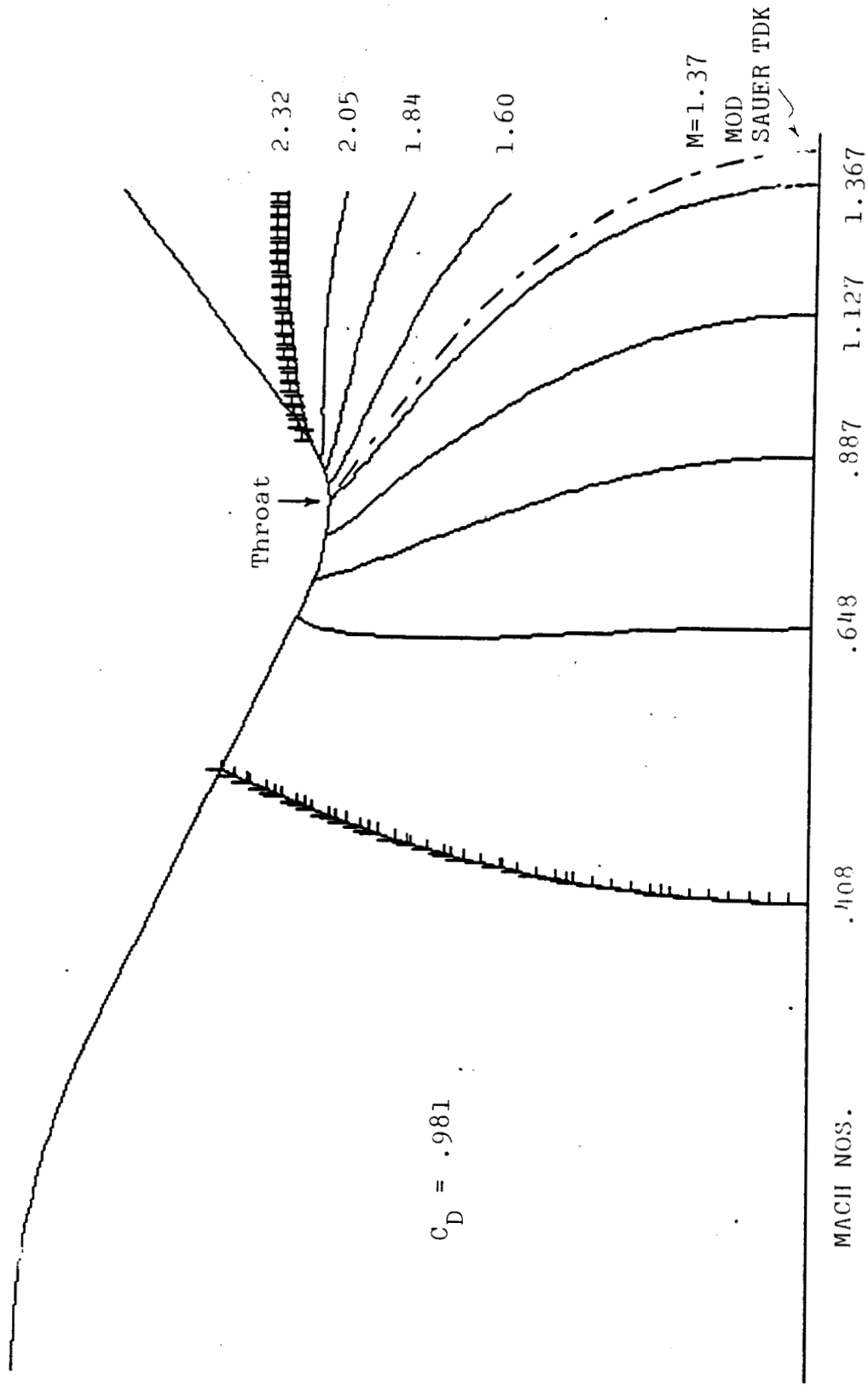


Figure 10: Isomach from Throat Minimum Point for Back Nozzle. (8)
Data and Predictions from TPk(1) and VNAP2. (7)

VNAP2 ISOMACHS
LARGE THROAT SSME



MACH NUMBER T=3.3052E-04 SEC
LOW VALUE= 1.6904E-01 HIGH VALUE= 2.5654E+00 LOW CONTOUR= 4.0867E-01
HIGH CONTOUR= 0.2326E+01 DELTA CONTOUR= 0.2396E+00
SSME LARGE THROAT DESIGN-EULER EQUATION SOLUTION (101X34) XE=3.5, FDT=.7

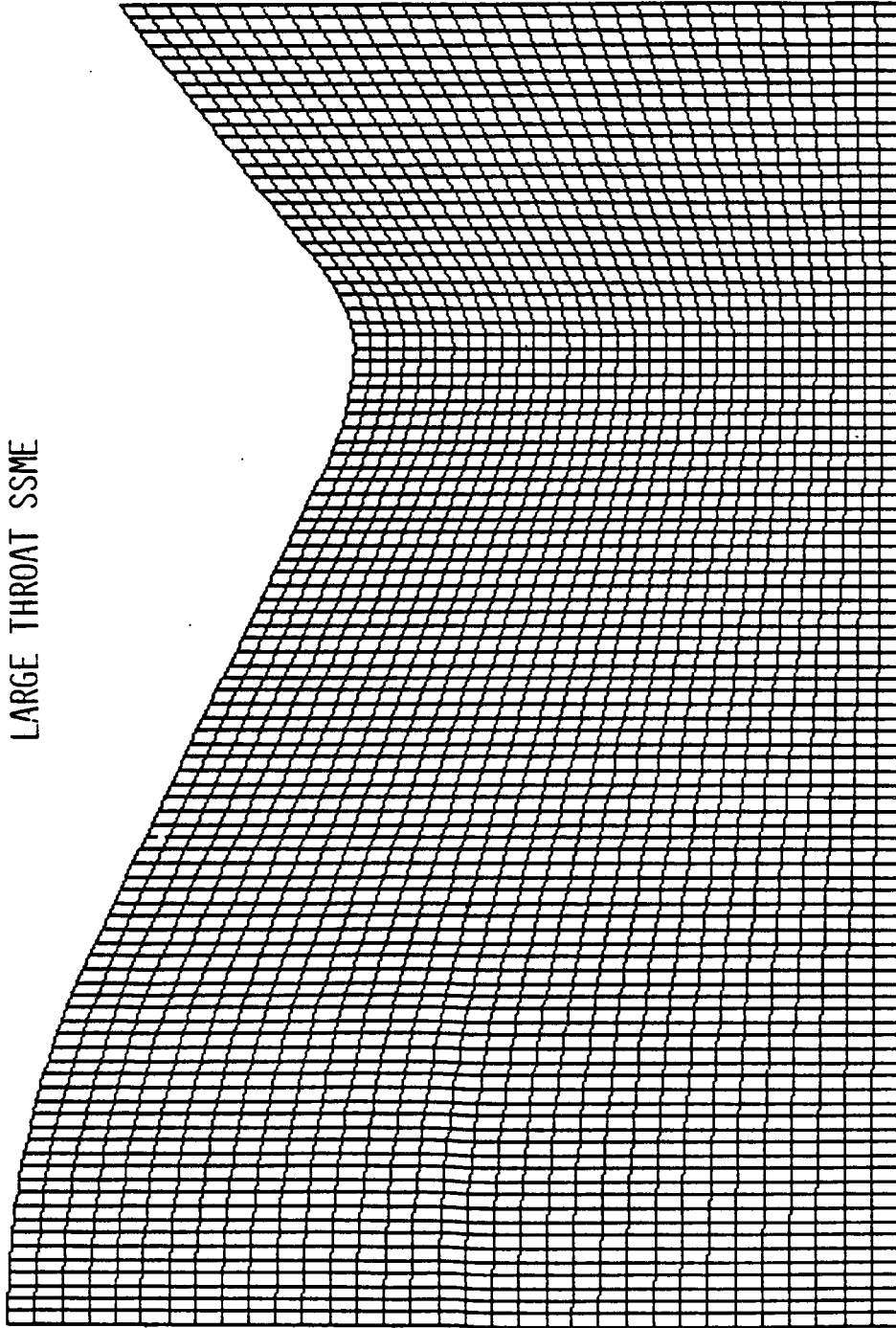
Figure 11: VNAP2 Isomach Predictions for the "Large Throat" SSME Design.
TJK Prediction shown for the Throat Minimum Point Isomach.

ORIGINAL PAGE IS
OF POOR QUALITY

VNAP2 SOLUTION GRID

101 x 34

LARGE THROAT SSME



ORIGINAL PAGE IS
OF POOR QUALITY

PHYSICAL SPACE GRID N= 3000 T=3.3052E-04 SEC
SSME LARGE THROAT DESIGN-EULER EQUATION SOLUTION (101X34) XE=3.5, FDT=.7

Figure 12: VNAP2 Solution Grid

SENSITIVITY OF MASS FLOW RATE TO FLOW ANGLE

$\gamma = 1.4$
 $R = .625$

$\theta(r)$	C_D	ΔC_D	NOTES
$\theta(r) = 0$.917		$C_D = \rho V$
$.9\theta(r)$.978	.061	
$\theta(r)$.986	.008	$C_{DMEASURED} = .985$
$1.1\theta(r)$.991	.005	
$\theta(r) = \phi - \frac{\pi}{2}$	1.269	.278	MAXIMUM C_D (WALL B.C. VIOLATED)

Figure 13: Sensitivity of Nozzle Mass Flow Coefficient, C_D , to Streamline Angle Variation

Figure 14:

TRANSONIC ANALYSIS
 COMPARISON OF TDK (MOD.SAUER) WITH VNAP2

CASE 1: BACK & CUFFEL, $R_U = .625$, $\gamma = 1.4$

	C_D	M_{WALL} $X=0$
VNAP2	.982	1.347
TDK	.986	1.346
EXPERIMENTAL	.985	1.346

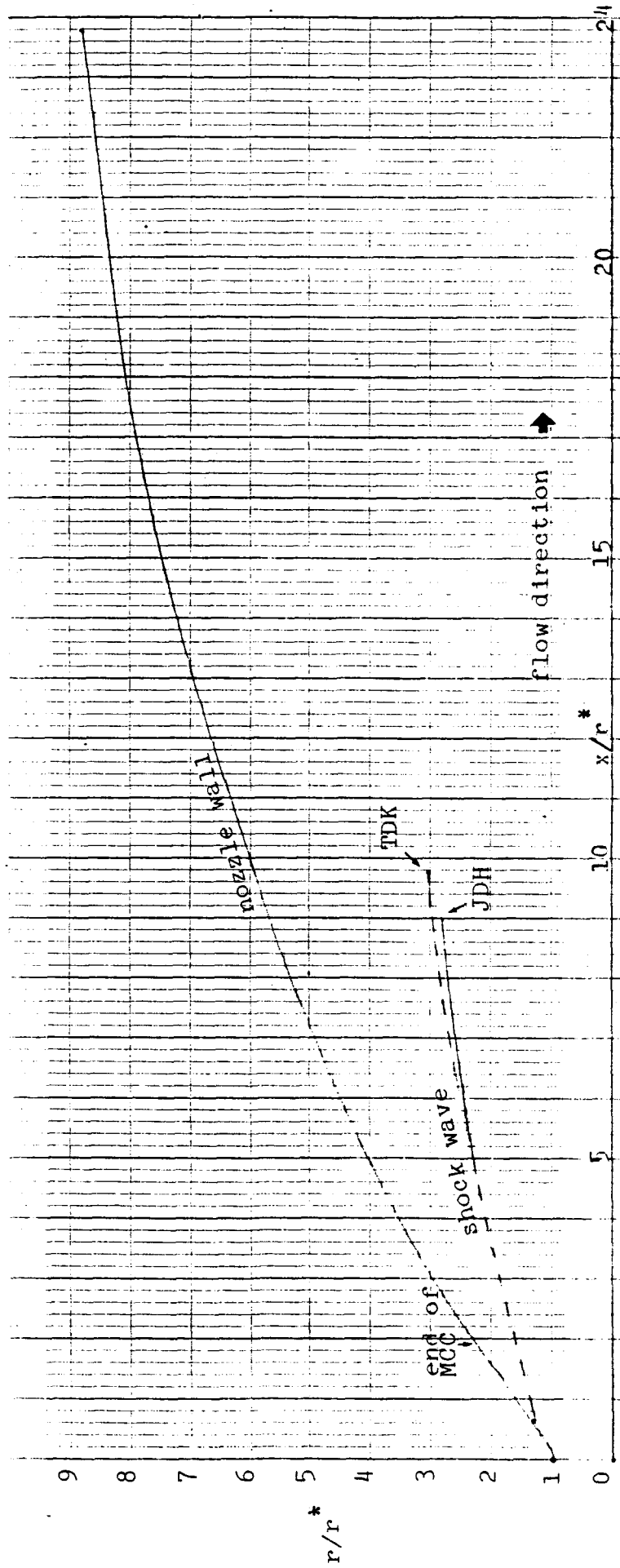
CASE 2: SSHE, CURRENT DESIGN, $R_U = 1$, $\gamma = 1.24$

VNAP2	.991	1.24
TDK	.991	1.23

CASE 3: SSHE, LARGE THROAT DESIGN, $R_U = .492$, $\gamma = 1.24$

VNAP2	.981	1.37
TDK	.983	1.37

JDH , Purdue Results , $\gamma=1.24$
 TDK , SEA Inc. Results , $\gamma 1.24$



ORIGINAL PAGE IS
 OF POOR QUALITY

Figure 15: SSME Current Design, Induced Shock Predictions

JDH, Purdue Results, $\gamma=1.24$
TDK, SEA Inc. Results, $\gamma=1.24$

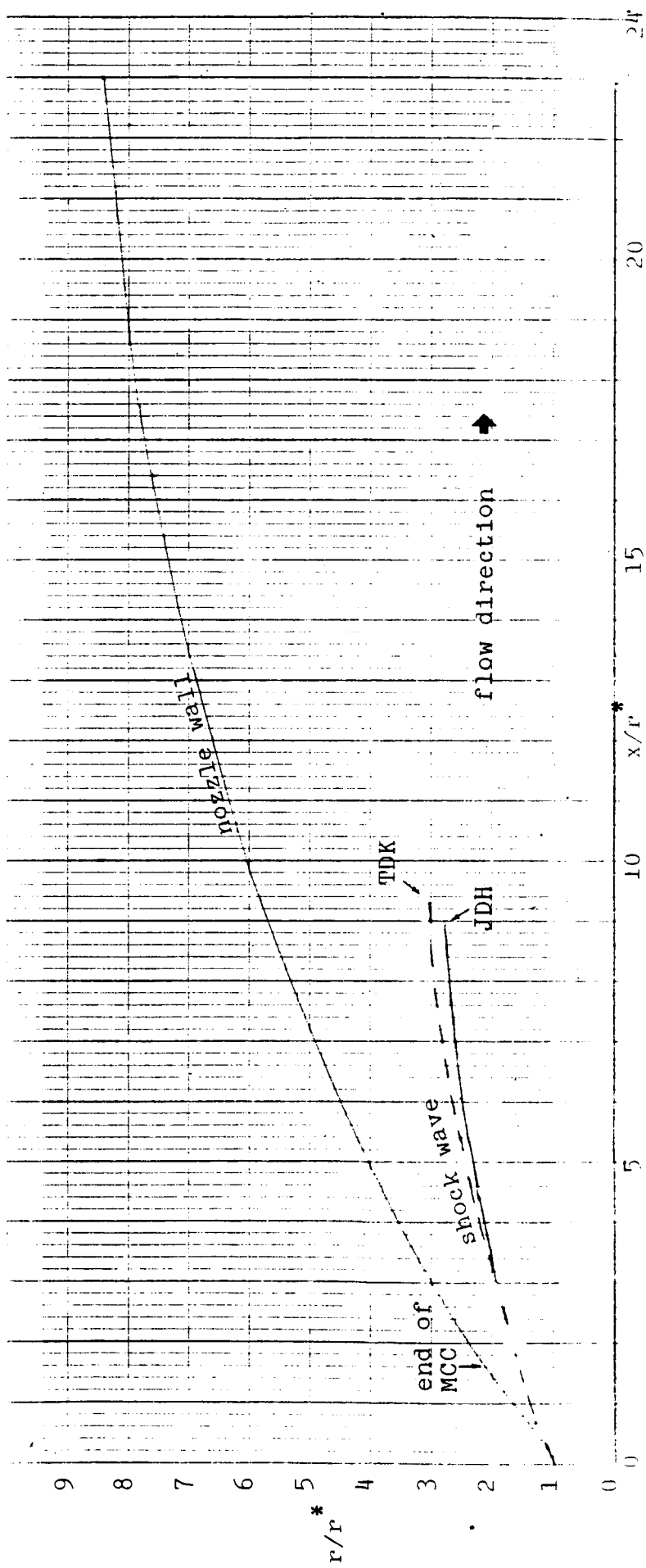


Figure 16: SSME "Large Throat" Design, Induced Shock Predictions

ORIGINAL PAGE IS
OF POOR QUALITY

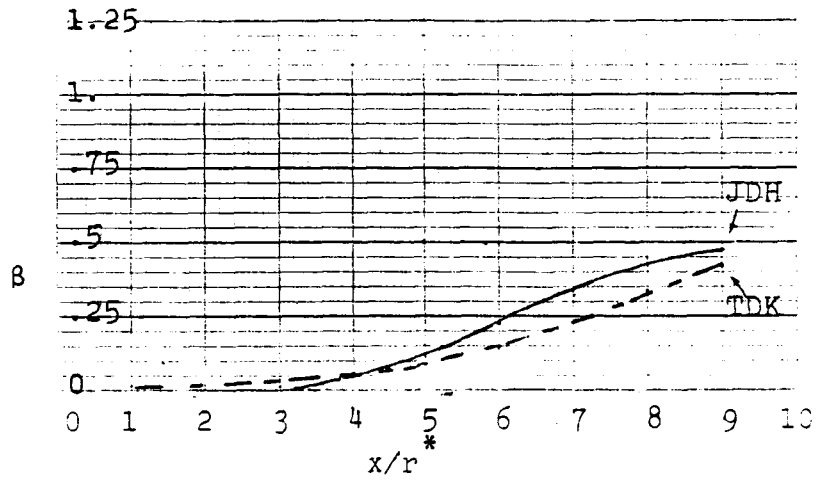


Figure 17: SSME Current Design
Shock angle vs x/r^*
 $\gamma=1.24$

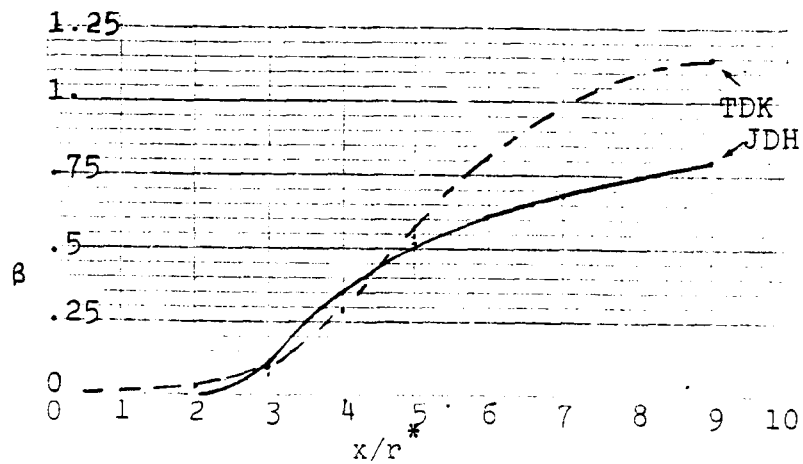


Figure 18: SSME "Large Throat" Design
Shock angle vs x/r^*
 $\gamma=1.24$

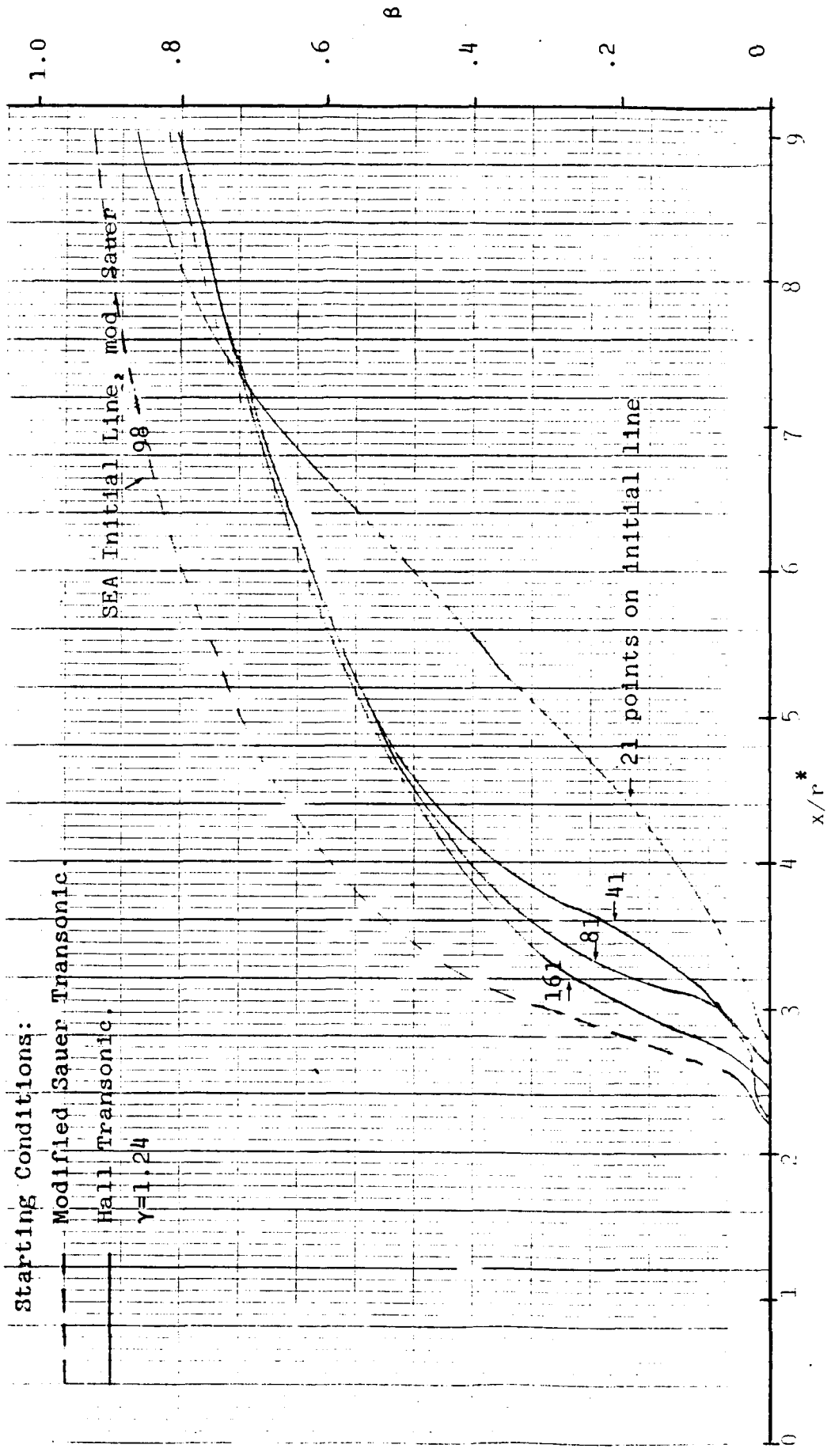


Figure 19: Shock Strength vs x/r^* for Differing Transonic Start Lines. "Large Throat" SSME Design.

Figure 20:

SUMMARY OF SHOCK STRENGTH PREDICTIONS

	$(P_2 - P_1) / P_1$ AT $X/R^* = 9$	NOTES
<u>CURRENT DESIGN</u>		
ROCKETDYNE	.43	EQUIL CHEM
LOCKHEED	.46	EQUIL CHEM
PURDUE (JDH)	.49	$\gamma = 1.24$, HALL TRANSONIC
SEA	.43	$\gamma = 1.24$, MOD SAUER TRANSONIC

LARGE THROAT DESIGN

ROCKETDYNE	.77	
LOCKHEED	.8	
PURDUE (JDH)	.8	as above
SEA	1.15	

$X/R^* = 9$ IS SHOCK POINT POSITION ON LAST LRC.

REFERENCES

1. Nickerson, G. R., Coats, D. E., and Dang, L. D., "The Two-Dimensional Kinetic (TDK) Reference Computer Program", Engineering and Programming Manual, Software and Engineering Associates, Inc., prepared for Contract NAS8-35931, NASA/MSFC, April 1985.
2. Nickerson, G. R. and Dang, Lanh D., Report No. SN76FR, "Assessment of the SSME Nozzle Performance" Software and Engineering Associates, Inc., prepared for Aerojet TechSystems Company, March 1985.
3. "JANNAF Rocket Engine Performance Prediction and Calculation Manual", CPIA 246, April 1975.
4. Hoffman, J. D., "A Computer Program for the Performance Analysis of Scarfed Nozzles", U.S. Army Missile Command Technical Report RK-CR-84-3, prepared for Propulsion Directorate, U.S. Army Missile Laboratory, May 1984.
5. TDK Data Package for the SSME, "Informal Communication from K. Gross", NASA/MSFC, received December 1984.
6. Carroll, R. G., et.al., "Performance Comparison of the Current SSME and a New Main Injector - Main Combustion Chamber Configuration Using the JANNAF Methodology", 22nd JANNAF Combustion Meeting, 7-10 October 1985.
7. Cline, M. C., "VNAP2: A Computer Program for Computation of Two-Dimensional, Time-Dependent, Compressible, Turbulent Flow", Los Alamos National Laboratory Report No. LA-8872, August, 1981.
8. Back, L. H., Massier, P. F., and Gier, H. L., "Comparison of Measured and Predicted Flows through Conical Supersonic Nozzles with Emphasis on the Transonic Region", AIAA Journal, Vol. 3, No. 9, Sept. 1965, pp. 1606-1614.
9. Hall, I. M., "Transonic Flow in Two-Dimensional and Axially-Symmetric Nozzles", Quarterly Journal of Mechanics and Applied Mechanics, Vol. XV, Pt. 4, 1962, pp. 487-508.
10. Smith, S. D., and Ratliff, A. W., "Rocket Exhaust Plume Computer Program Improvement, Vol. I, Final Report" LMSC-HREC D162220-I, prepared for Contract NAS7-761, June 1971.
11. Private communication from R. O'Leary, Rocketdyne Division of Rockwell International, October 1985.

12. Lee, Y. C., "Nozzle Flowfield and Specific Impulse (Isp) Calculations for Rocketdyne's Shock Free Large Throat SSME Nozzle" NASA MSFC, memo ED33(45-85), September 25, 1985.
13. Rao, G. V. R., "Exhaust Nozzle Contours for Optimum Thrust", Jet Propulsion, Vol. 28, No. 6, June 1958, pp. 377-382.

APPENDIX A

DISCUSSION OF SUMMARY OUTPUT

At the end of each computer run, the TDK program prints a table of summary output. Examples of this output are given in Figures 6 and 7. The first item printed is the title

TDK PERFORMANCE SUMMARY: (title)

Next, performance parameters summarizing the results of the calculations are printed in three columns. The left hand column identifies each item to be printed and its units. The first column of results is for the first MOC/BLM solution, and second column of results is for the second MOC/BLM solution.

The items labeled ISP(TDK), THRUST(TDK), WDOT(TDK), CD, CSTAR(TDK), and CF(TDK) are defined as:

<u>Name</u>	<u>Units</u>	<u>Definition</u>
ISP(TDK)	sec	Specific Impulse, $I_{sp,2D}$
THRUST(TDK)	lbf	Thrust, F_{2D}
WDOT(TDK)	lbm/sec	Mass Flow, \dot{m}_{2D}
CD	-	Flow coefficient, $C_{D,2D}$
CSTAR(TDK)	ft/sec	Characteristic Velocity, C^*_{2D}
CF(TDK)	-	Thrust coefficient, $C_{F,2D}$

If a TDF or TDE calculation was made rather than TDK, then these items will be relabeled.

The values given for $I_{sp,2D}$ and m_{2D} are obtained by evaluating the integrals discussed in the documentation for MOC module subroutine CHAR. The mass flow integral is evaluated across the MOC initial data line. The I_{sp} integral is evaluated across the initial data line, plus the integral of the axial component of wall pressure from the initial data line to the nozzle end point. The thrust is

$$F_{2D} = I_{sp,2D} \dot{m}_{2D}$$

The nozzle flow coefficient is calculated as

$$C_{D,2D} = \dot{m}_{2D} / \dot{m}_{1D}$$

where

$$\dot{m}_{1D} = \rho_{1D}^* V_{1D}^* A^*$$

is obtained from ODE. A^* is the geometric throat area.

The characteristic velocity, C^* , is calculated as

$$C_{2D}^* = I_{sp,2D} g / C_{F,2D}$$

where the thrust coefficient, C_F , is defined by

$$C_{F,2D} = F_{2D} / P_c A^*$$

Again, A^* , is the geometric throat area.

The items labeled DISP(BLME), DFOPT(BLME), DF(BLME), ISP(TC), THRUST(TC), and CF(TC) are defined as follows:

<u>Name</u>	<u>Units</u>	<u>Definition</u>
DISP(BLME)	sec	$\Delta I_{sp,BLM}$
DFOPT(BLME)	lbf	ΔF_{BLM} for $P_e = P_{amb}$
DF(BLME)	lbf	ΔF_{BLM}

851106

<u>Name</u>	<u>Units</u>	<u>Definition</u>
ISP(TC)	sec	$I_{sp,2D,BLM}$
THRUST(TC)	lbf	$F_{2D,BLM}$
CF(TC)	-	$C_{F,2D,BLM}$

In the above, the thrust loss calculated by the BLM is given by the following relation:

$$\Delta F_{BLM} = 2\pi r_e \cos \alpha_e * \rho_e U_e^2 \theta_{BLM} - 2\pi r_e \cos \alpha_e * (P_e - P_{amb}) \delta_{BLM}^*$$

The additional items, printed are

$$\begin{aligned} \Delta I_{sp,BLM} &= \Delta F_{BLM} / \dot{m}_{2D} \\ I_{sp,2D,BLM} &= (F_{2D} - \Delta F_{BLM}) / \dot{m}_{2D} \\ F_{2D,BLM} &= F_{2D} - \Delta F_{BLM} \\ C_{F,2D,BLM} &= F_{2D,BLM} / P_c A^* \end{aligned}$$

Performance parameters summarizing the results of the second MOC/BLM calculation differ from the first set printed as follows:

- 1) The TDK and ODE results for the second (inviscid core) run have a modified wall contour, throat area, and expansion ratio. Note that the system enthalpy is different than used in the first run if the BLM wall calculation is not adiabatic.
- 2) The BLM results are re-calculated using edge conditions from the second TDK run. BLM itself is not re-run, and the values of δ^* and θ are not changed.

The equations used are the same as given above.